Supplemental Figure 1

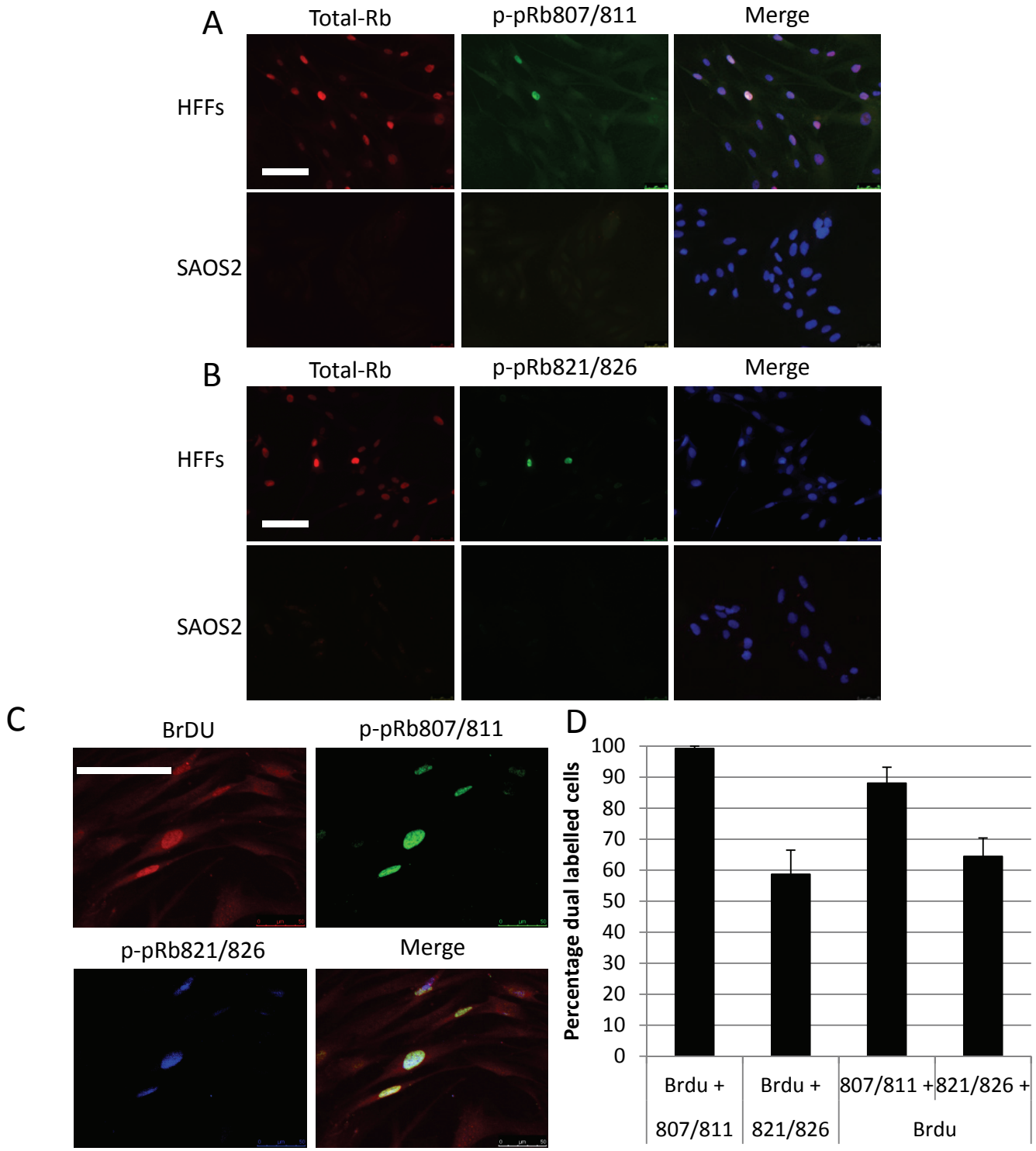

Supplemental Figure 1: Antibody specificity tests. (A) Isolated fibroblasts and Rb-null SAOS2 cells were stained with antibodies raised against the Rb protein and Rb phosphorylated at serine residues 807 and 811, only a small proportion of cells stain with both the total Rb and the p-pRb807/811. SAOS2 cells did not stain positive for either antibody (B) Cells were stained as in A but using an antibody raised to Rb phosphorylated at threonine residues 821 and 826. (C) Fibroblasts pulsed with Brdu were co-stained to detect Brdu incorporation and phosphorylation of Rb at residues 807/811 and 821/826. D)Percentages of Brdu positive cells with phospho-Rb staining and also percentages of phospho-Rb positive cells which are Brdu positive. Error bars represent standard deviation. Scale bars represent 100 µm.

Supplemental Figure 2

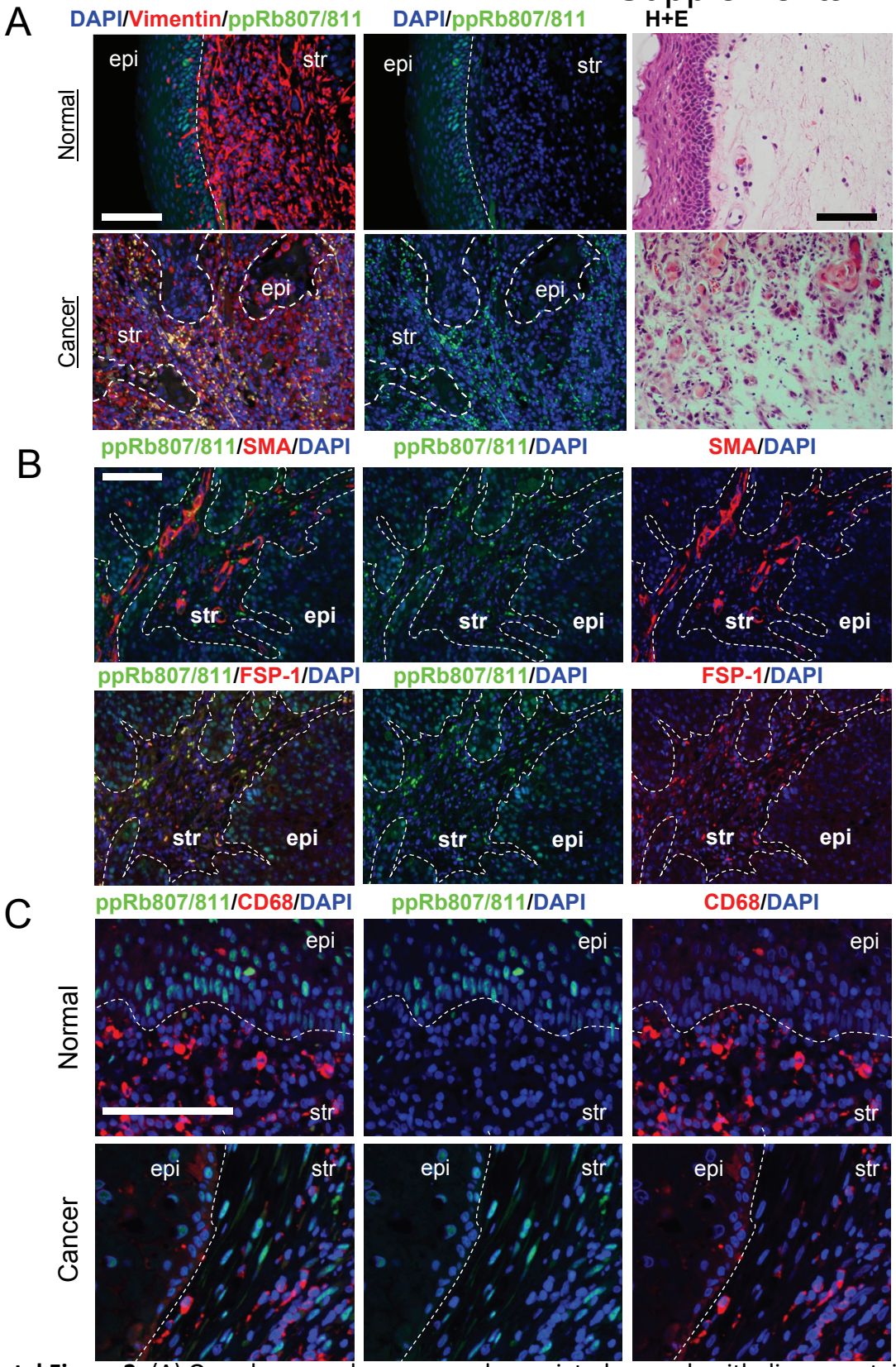

Supplemental Figure 2: (A) Oro-pharyngeal cancers and associated normal epithelia were stained using antibodies against phosphorylated Rb (ppRb807/811) and the stromal marker vimentin. The stroma associated with cancerous epithelium stained positively for ppRb807/811. (B) Stromal ppRb807/811 staining co-localised with the Fibroblast specific protein (FSP1) but not with smooth muscle actin (SMA). (C) ppRb807/811 infrequently co-stained with the macrophage marker CD68. in either normal or cancer associated stroma. Scale bars represent 100 μm.

Supplemental Figure 3

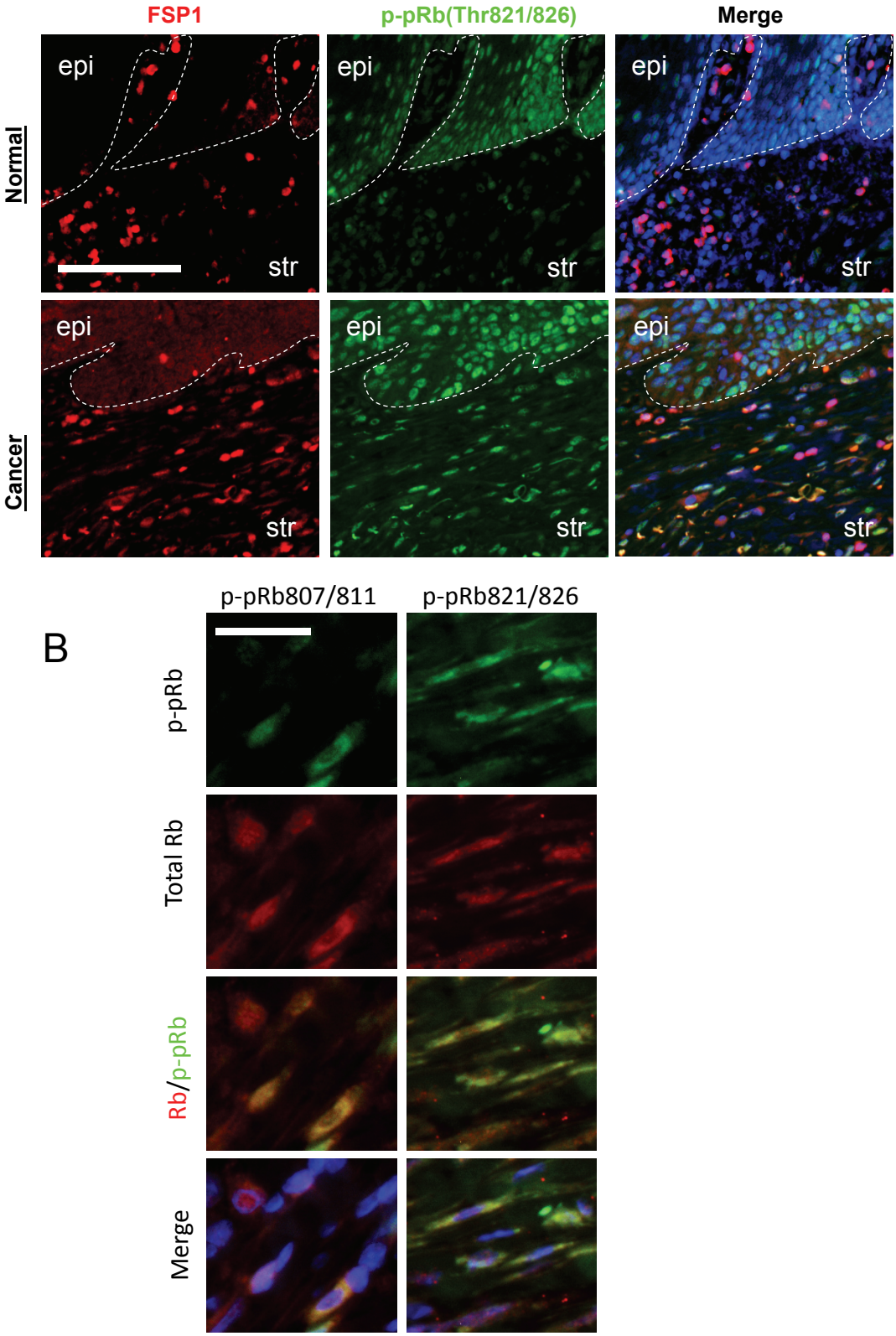

Supplemental Figure 3: (A) Oro-pharyngeal cancers and associated normal epithelia were stained using antibodies against phosphorylated Rb (ppRb821/826) and FSP1. ppRb821/826 frequently co-localised with FSP1 in the stroma associated with cancerous epithelium. Scale bars represent 100 µm. (B) Mis-localisation of the Rb protein is observed when phosphorylated Rb is detected in the cytoplasm, residual Rb protein is detected in he nuclei of some cells. Scale bars represent 25 µm.

Supplemental Figure 4

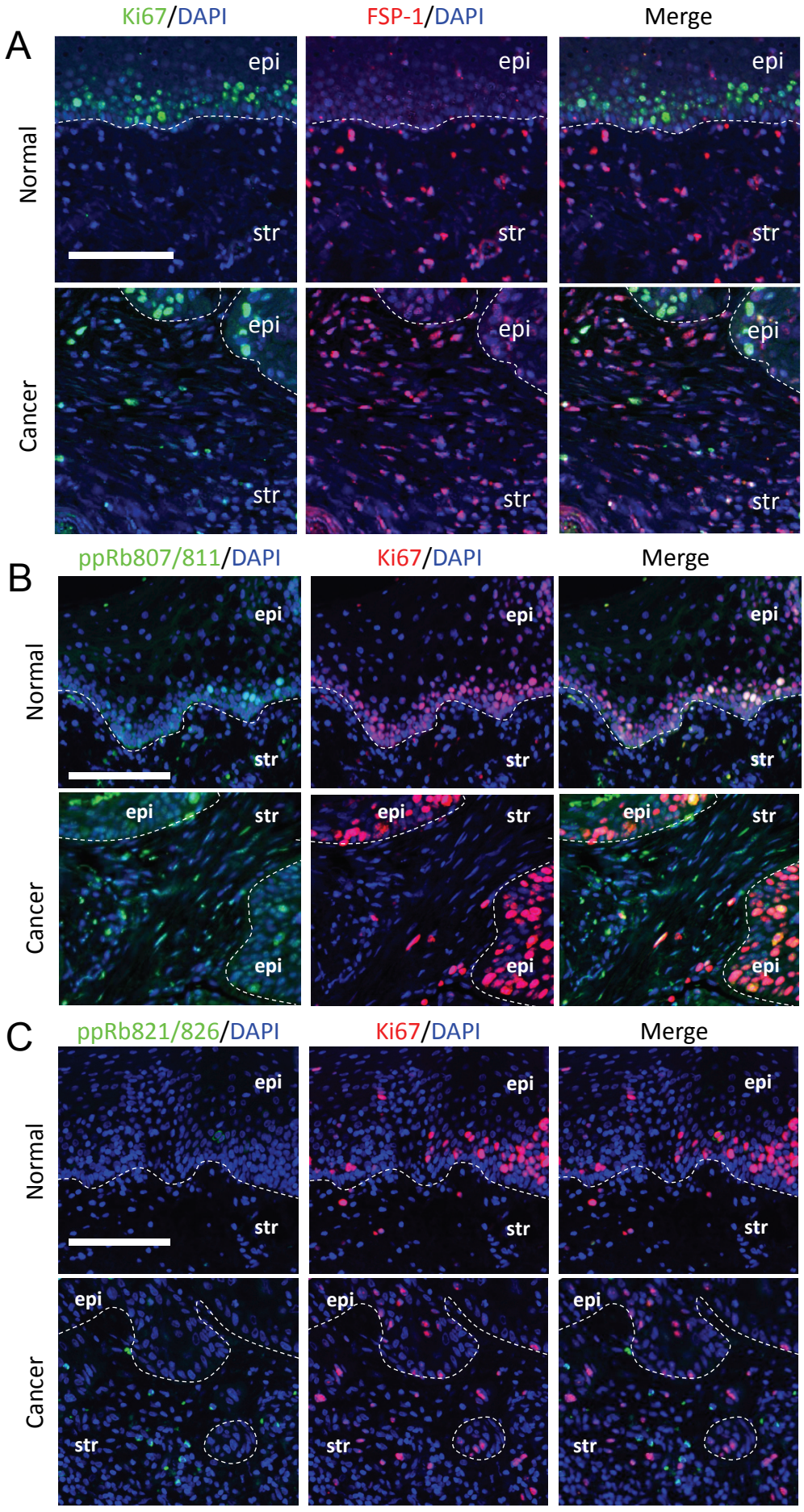

Supplemental Figure 4: Ki67 staining in the stroma of oro-pharyngeal cancers. (A) Ki67 staining was strongly detected in the majority of normal and cancerous epithelium, the staining in the stromal compartment was much less frequent, across 33 cancer samples tested an average of 13% of FSP1 positive cells also stained positively for Ki67. Costaining of stroma associated with normal and cancerous epithelium with Ki67 and p-pRb807/811 (B) or p-pRb821/826 (C) identified that a large proportion of stromal cells that are positive for phosphorylated Rb are not Ki67 positive. Scale bars represent 100 μm.

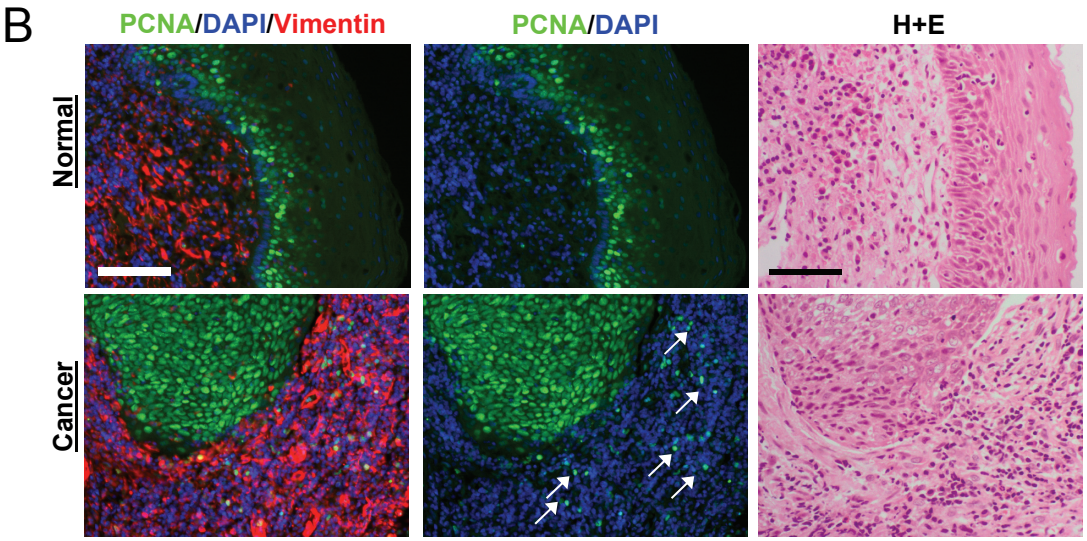

Supplemental Figure 5: Enhanced PCNA staining within the stroma associated with oro-pharyngeal cancers. Expression of the stromal marker vimentin and PCNA were assessed in oro-pharyngeal cancer specimens and matched normal tissue. PCNA was detected strongly in basal and supra-basal epithelial cells, but only in a small number of stromal cells in normal tissue. In comparison, almost all epithelial cells in cancerous regions stained positive for PCNA and it was readily detected in the stroma associated with the cancer epithelium. Scale bars represent 100 μm.

Supplemental Figure 6

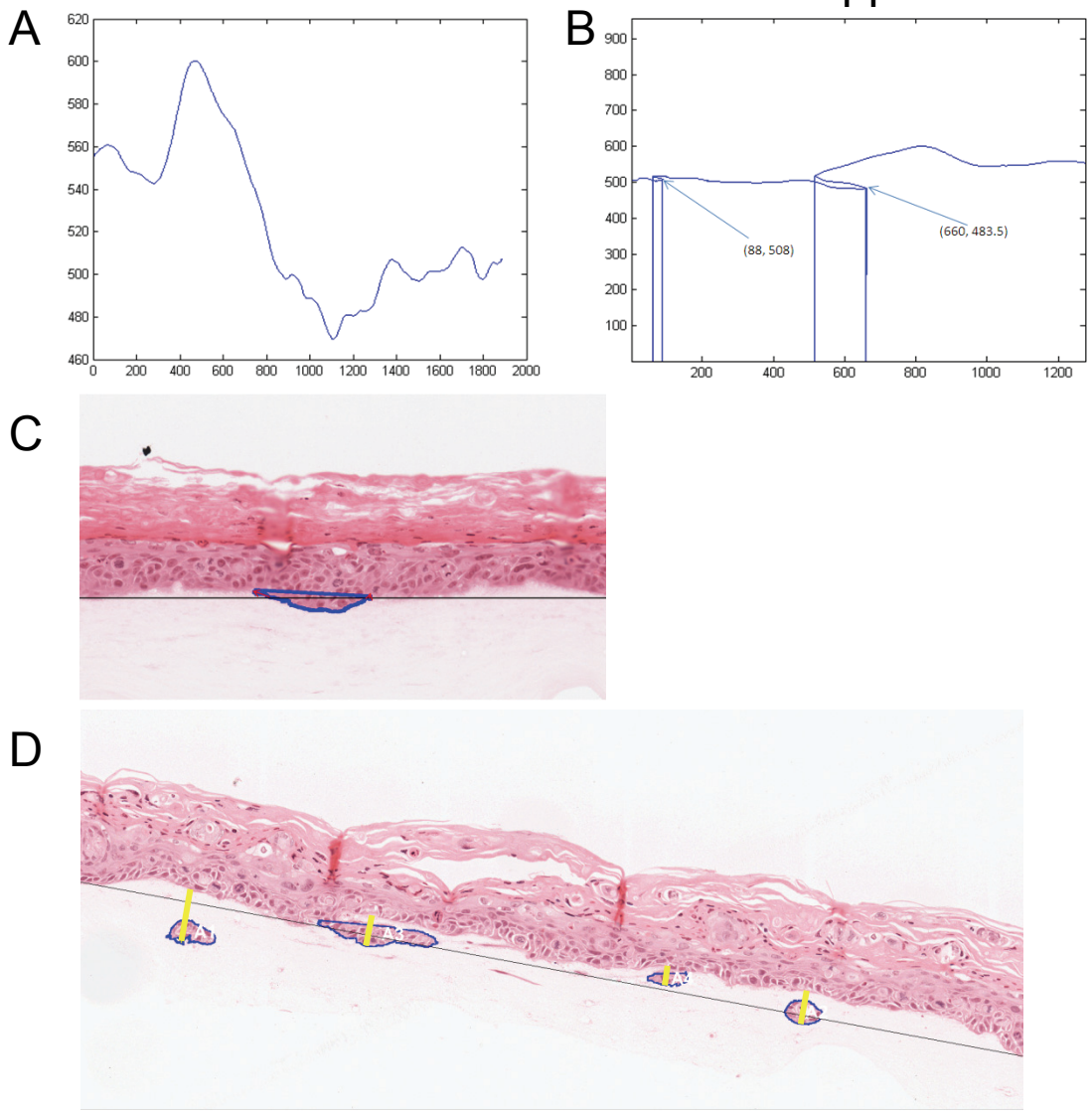

Supplemental Figure 6: A) A plot of the *x* coordinate which is used to determine any changes in direction (turning points) in the lower tissue boundary. B) a plot of the *x* and *y* coordinates of a sample image. This plot shows the lower boundary, however it appears reversed as Matlab's image coordinate system is ordered from top to bottom and left to right, whereas this plot uses the standard coordinate system for graphs (where all values are positive). The turning points and are highlighted and the trigonometric point to point gradient of these points (as a straight line) is reflected to determine the extent of the invasion. C) To identify invasions which were apparent but not characterized by turning points, as in A), the baseline line, marked in black, is taken as the lower left and right point of the main section of tissue. This requires the image to be sectioned in such a way that only a reasonably straight area of tissue is being examined). The figure shows a large area that passes the baseline; this area is therefore considered invasive. The algorithm then scans the boundary in each direction to determine where the gradient levels out (marked by red arrows). These points are then marked as the left and right upper areas of the invasion. D) The depth of the invasion is determined following the identification of invasive regions. The invasive areas are scanned at an angle perpendicular to the baseline from the leftmost to the rightmost points of the invasion to determine the furthest point from the main tissue area. This marked by the yellow line in the figure.

Supplemental Figure 7

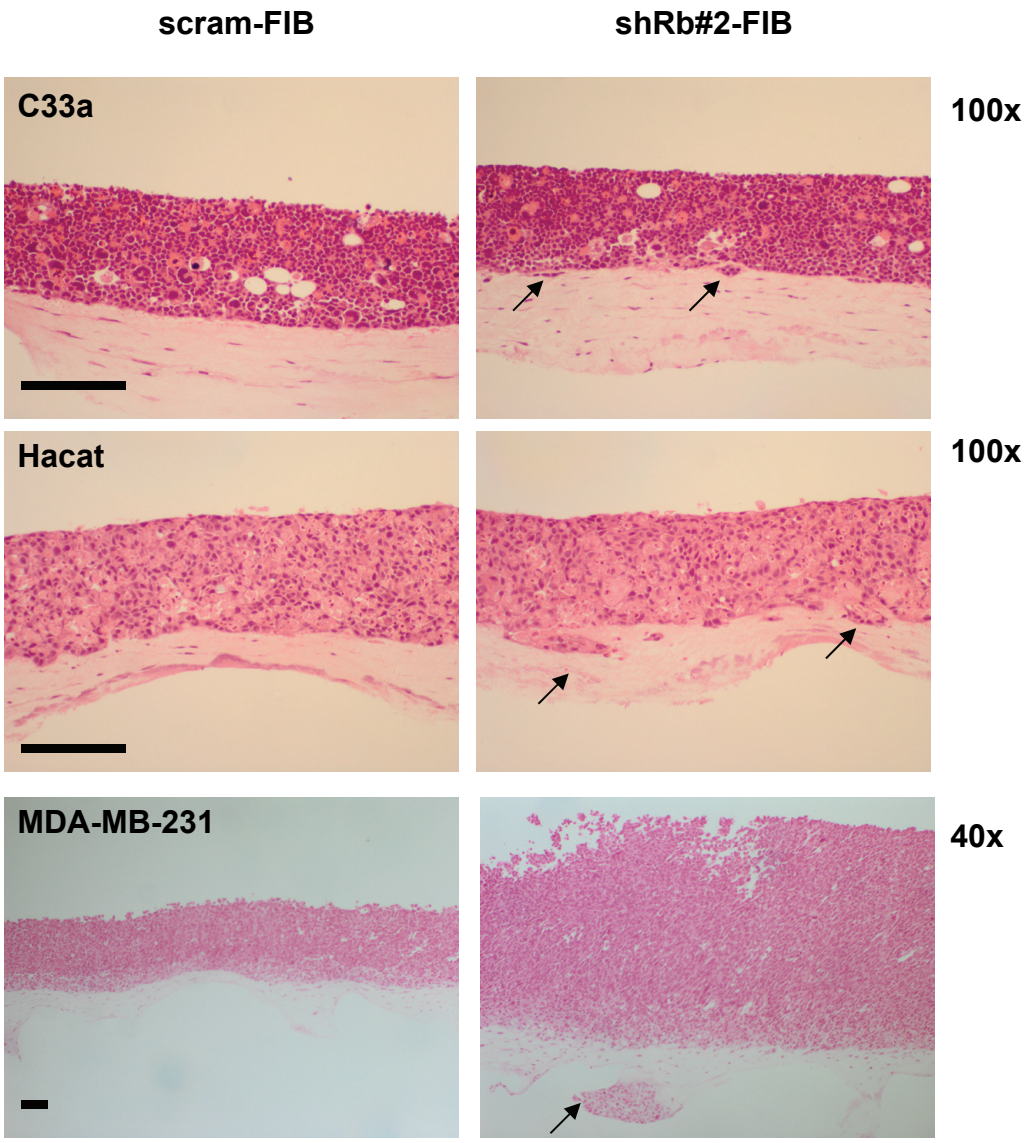

Supplemental Figure 7: Rb-depleted fibroblasts promote invasion by various epithelial cell lines. Organotypic raft cultures of the cervical cancer cell line C33a, the immortalised keratinocyte cell line, HaCat, and the breast cancer cell line MDA-MB-231 show that when cultured with Rb-depleted fibroblasts the epithelial cells are promoted to invade into the collagen plug. Culturing MDA-MB-231 cells with Rb-depleted fibroblasts also resulted in a two-fold increase in epithelial thickness. Invasive events are indicated by arrows. Scale bars represent 100 μm.

Supplemental Figure 8

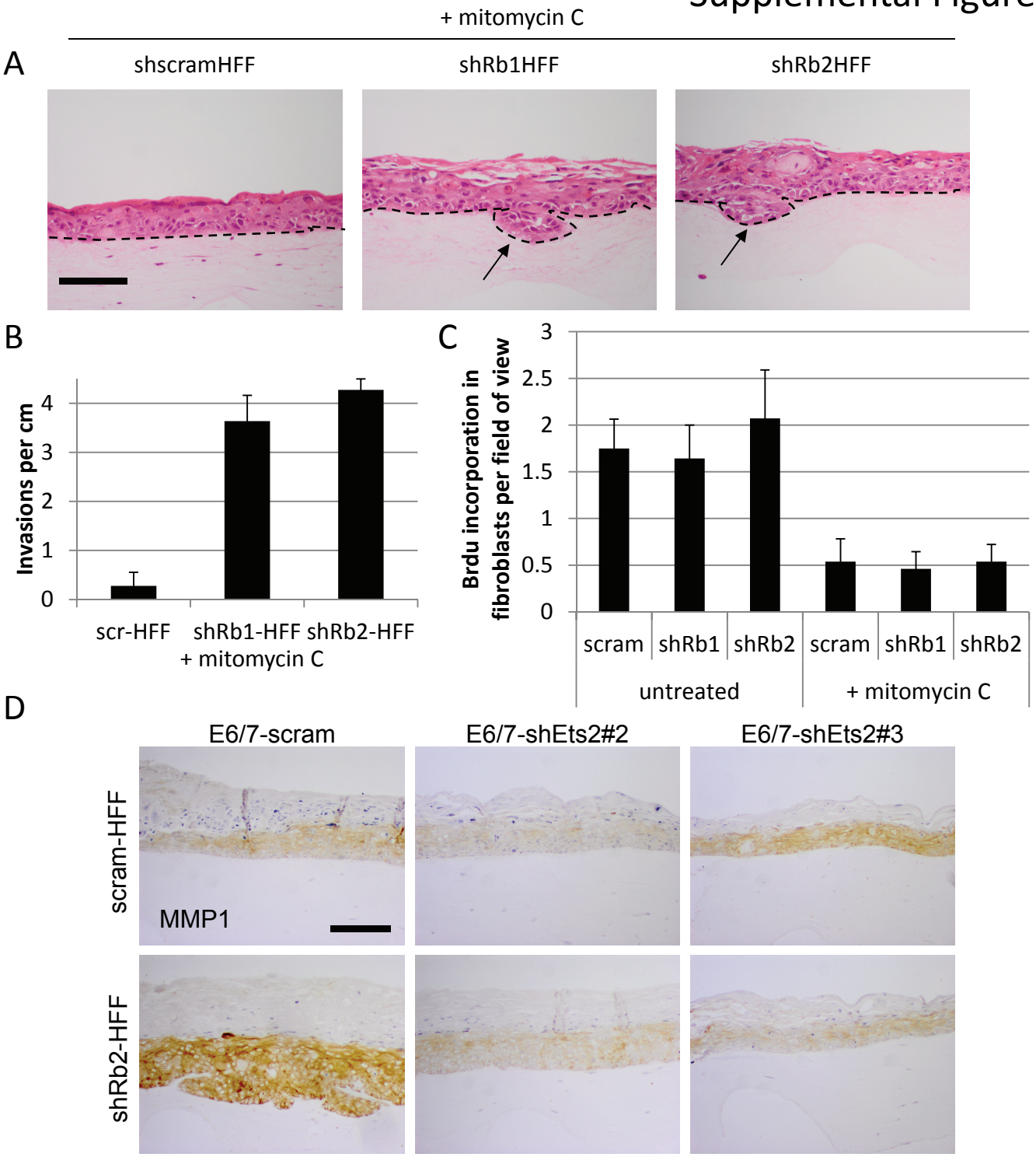

Supplemental Figure 8: (A) Mitomycin treatment of fibroblasts prior to incorporation into organotypic cultures does not alter the invasive phenotype of epithelium cultured with Rb-depleted fibroblasts. (B) The frequency of epithelial invasions in the organotypic cultures shown in A. Error bars represent standard deviation. (C) The frequency of Brdu-incorporation in collagen embedded fibroblasts from organotypic cultures. Error bars represent standard deviation. (D) Retroviral knockdown of Ets2 in the epithelium. Culturing control epithelium with Rb-depleted fibroblasts resulted in an invasive epithelium with strong MMP1 staining. Reduction of Ets2 levels in the epithelium reduced both MMP1 staining and the number of invasive events. Scale bars represent 100 µm.

Supplemental Table 1-
Scores of phospho-Rb (Thr821/826) staining in the stroma of matched normal and cancerous Head and Neck epithelium

Sample	Normal stroma p-pRb	Normal stroma (FSP1/p-pRb)*	Cancer stroma p-pRb	Cancer stroma (FSP1/p-pRb)*	HPV Status
1	+	+	+++	+++	-
2	++	+	+++	+	-
3	++	+	++	+++	+
4	++	+	+++	++	-
5	++	+	+++	+++	+
6	n/a	n/a	+++	+++	-
7	++	+	+++	+++	-
8	n/a	n/a	+++	+++	-
9	++	+	+++	+++	-
10	+	++	+++	++	-
11	+	+	+++	+++	-
12	+	+	+++	+++	-
13	n/a	n/a	+++	+++	-
14	n/a	n/a	+++	+++	+
15	+	++	+++	+++	-
16	n/a	n/a	++	+++	-
17	++	++	+++	+++	-
18	n/a	n/a	+++	+++	+
19	++	++	+++	+++	-
20	+	++	+	+	-
21	++	+++	+++	+++	-
22	+	+	++	+++	-
23	+	+	++	+++	-
24	++	+++	+++	+++	-
25	++	++	+++	+++	-
26	n/a	n/a	++	+++	-
27	+	+	++	+++	-
28	+	+	+++	+++	-
29	+	+	++	++	-
30	+	+	+++	+++	-
31	n/a	n/a	+++	+++	-
32	+ (**)	++ (**)	+++	+++	-
33	+	+	++	+++	-
34	++ (**)	++ (**)	+++	+++	-

*+++ indicates >75% FSP1 positive fibroblasts are p-pRb positive, ++ indicates 25-75% FSP1 positive fibroblasts are p-pRb positive, + indicates 10-25% FSP1 positive fibroblasts are p-pRb positive and - indicates <10% FSP1 positive fibroblasts are p-pRb positive
** Indicates normal tissue within close proximity to cancerous epithelium

Supplemental Methods

Detection of invasion

Whole Slide Images (WSI) were obtained using an Aperio ScanScope CS Slide Scanner at a magnification of x40. Images were automatically thresholded using Otsu's technique (Otsu, 1979). A binary image was then constructed using the resulting image matrix. The lower area of the binary image output is the area examined, as the algorithm assumes that when the image is extracted from the WSI that it will be orientated in such a way that invasion will be apparent on the lower edge of the tissue sample. Using the rules of trigonometry, the *x* coordinates of the lower boundary were extracted, smoothed using a linear filter and plotted (Supplemental Figure 6A). The indexes of the turning points (that are subject to a threshold of 150 consecutive coordinate points, so that minor changes are not detected) correspond to the actual *x* index in the image, this in turn allows the *y* index in the image to found (Supplemental Figure 6B).

For regular shaped invasions (i.e. do not have inlets into the main tissue section) a baseline is defined and where the tissue passes the base line, the area will be regarded as invasive if the area of tissue that passes the baseline is above a given threshold (in the case below this was set to > 3000 pixels). To determine where the invasion starts, starting from the left or right point of the area under consideration on the base line, the algorithm scans up until the gradient levels out (Supplemental Figure 6C).

To determine the depth of the invasion, the line perpendicular to the baseline is scanned through the area of interest to determine the thickest point. As the gradient of the baseline determines the direction of the tissue, the perpendicular gradient is

regarded as the direction the invasion would travel in. This is shown in Supplemental Figure 6D.

The trigonometric point to point distance is taken of the top and bottom points illustrated in Supplemental Figure 6D. Areas that appear to be separate from the main tissue body are separate entities and are simply determined by using the label matrix function bwlabel in Matlab. Only areas that are > 3000 pixels in size and are below the main tissue body are regarded as valid. To determine the distances in microns, the Aperio Scanner outputs a ratio between pixels and microns. In the samples that were taken in this experiment, the microns per pixel (MPP) was 0.2517 MPP.

Supplemental References:

Otsu, N. (1979). A Threshold Selection Method from Gray-Level Histograms. Systems, Man and Cybernetics, IEEE Transactions on *9*, 62-66.